Generation of a physiological sympathetic motor rhythm in the rat following spinal application of 5-HT

Nephtali Marina, Melody Taheri and Michael P. Gilbey

Department of Physiology, University College London, Hampstead Campus, London NW3 2PF, UK

When applied *in vitro* to various CNS structures 5-HT and/or NMDA have been observed to generate rhythmic nervous activity. In contrast, reports of similar *in vivo* actions are relatively rare. Here we describe a physiological sympathetic motor rhythm regulating the thermoregulatory circulation of the rat tail (T-rhythm; 0.40–1.20 Hz) that can be elicited following intrathecal (I.T.) application of 5-HT to an *in situ* 'isolated' spinal cord preparation (anaesthetized rats spinalized at T10–T11 and cauda equina cut). I.T. injections were delivered to L1 as sympathetic neuronal activity to the tail (SNAT) arises from preganglionic neurones at T11–L2. SNAT was abolished after spinal transection ($n = 18$) and it did not return spontaneously. The administration of 5-HT (250 nmol) generated rhythmic sympathetic discharges ($n = 6$). The mean frequency of the T-like rhythm during the highest level of activity was 0.88 ± 0.04 Hz which was not significantly different from the T-rhythm frequency observed in intact animals (0.77 ± 0.02 Hz; $P > 0.05$ $n = 16$). In contrast, NMDA (1 μmol) generated an irregular tonic activity, but it failed to generate a T-like rhythm ($n = 9$), even though the mean levels of activity were not significantly different to those produced by 5-HT. However, 5-HT (250 nmol) applied after NMDA generated a T-like rhythm (0.95 ± 0.11 Hz, $n = 6$). Our observations support the idea that 5-HT released from rostral ventromedial medullary neurones, known to innervate sympathetic preganglionic neurones, can induce sympathetic rhythmic activity.

(Received 25 October 2005; accepted after revision 4 January 2006; first published online 5 January 2006)
Corresponding author M. P. Gilbey: Department of Physiology, University College London, Hampstead Campus, London NW3 2PF, UK. Email: m.gilbey@ucl.ac.uk

Rhythmic activity is associated with many nervous system functions, i.e. sensory (Buzsáki & Draguhn, 2004), cognitive (Ward, 2003), somatomotor (Arshavsky, 2003) and autonomic motor (Malpas, 1998; Gilbey, 2001). In some cases the purpose of such patterning of activity is obvious, as with the motor outputs generating movement. In cases where the function of rhythmic activity is unclear it has been proposed that it reveals a mechanism whereby pools of neurones can form the dynamic networks required for various nervous system processes (Singer, 1993; Gilbey, 2001).

Data from *in vitro* studies have demonstrated that NMDA and 5-HT can cause single neurones (conditional pacemakers) and neuronal networks to generate rhythmic activity (Arshavsky, 2003), i.e. fictive locomotion generated following activation of NMDA receptors (Alford *et al.* 2003) and/or 5-HT receptors (Schmidt & Jordan, 2000); fictive sucking and mastication subsequent to activation of NMDA receptors (Nakamura *et al.* 2004*a*); rhythmical activity in sympathetic preganglionic neurones (Pickering *et al.* 1994) and fictive respiratory activity in the pre-Bötzinger complex (Peña & Ramirez, 2002) elicited by 5-HT receptors. Attempts to pharmacologically generate rhythmic neural activity *in vivo* are less common and have focused on locomotor outflows. Such studies show that intrathecal (I.T.) administration of NMDA consistently elicits fictive locomotion in decerebrate neuromuscularly blocked adult cats and marmoset monkeys, similar to that evoked by electrical stimulation of the mesencephalic locomotor region (Douglas *et al.* 1993; Fedirchuk *et al.* 1998). In comparison, 5-HT is less effective (Fedirchuk *et al.* 1998).

In the present study we aimed to generate a physiological sympathetic motor rhythm in an *in situ* 'isolated' spinal cord preparation (anaesthetized rats spinalized at T10–T11 and cauda equina cut) by the I.T. application of NMDA and/or 5-HT. For this purpose, we used a rat tail circulation model (Johnson & Gilbey, 1994). In anaesthetized intact preparations, we have observed robust rhythmicity in single and population postganglionic neuronal discharges supplying the rat tail circulation (T-rhythm, 0.40–1.20 Hz; Johnson & Gilbey, 1996; Smith & Gilbey, 2000). We have proposed that rhythmic activity arises from a family of weakly coupled or uncoupled oscillators that can be reset or entrained by various synaptic inputs (Chang *et al.* 1999, 2000; Staras *et al.* 2001). We have yet to identify the nervous

 DOI: 10.1113/jphysiol.2005.100677

substrate(s) that generates the T-rhythm, although we have evidence that it is generated within the CNS below the collicular level (Smith & Gilbey, 2000; Collins & Gilbey, 2003). The sympathetic preganglionic neurones driving SNAT receive vital inputs from neurones within the rostral ventromedial medulla (RVMM) (Rathner *et al.* 2001; Tanaka *et al.* 2002; Korsak & Gilbey, 2004; Ootsuka *et al.* 2004; Ootsuka & Blessing, 2005; Ootsuka & McAllen, 2005), some of which contain 5-HT and/or v-glut3 transporter (Smith *et al.* 1998; Nakamura *et al.* 2004*b*). Here we test the hypothesis that the T-rhythm can be generated within the spinal cord and can be driven by 5-HT and/or NMDA. Some of the data have been published previously in abstract form (Marina & Gilbey, 2005*a*,*b*).

Methods

General preparation and maintenance

Experiments were performed on 18 male Sprague–Dawley rats (280–320 g, bred in-house at UCL) and carried out in accordance with the UK Animals (Scientific Procedures) Act 1986 and associated guidelines. Animals were anaesthetized with 20% urethane ($1.3\,g\,kg^{-1}$ I.P., supplemented with 5–10 mg I.V. as required). The depth of anaesthesia was monitored using stability of blood pressure, corneal reflexes and flexor responses to paw-pinch. Animals were neuromuscularly blocked before spinal cord transection (SCT) with a single dose of Pancuronium Bromide (Pavulon, Faulding Pharmaceuticals, plc, Warwickshire, UK; $1\,mg\,kg^{-1}$ I.V.). During this period (approximately 30 min) the depth of anaesthesia was assessed from the stability of blood pressure and heart rate.

The trachea was cannulated and tracheal pressure was monitored. Animals were vagotomized and ventilated artificially with O_2-enriched air. The right femoral vein and artery were cannulated to allow I.V. administration of drugs and monitoring of mean blood pressure (MABP), respectively. Animals were maintained in central apnoea so that the T-rhythm would not be entrained to central respiratory drive (CRD; Chang *et al.* 1999). Central apnoea was induced by hyperventilation hypocapnia and was monitored by recording the diaphragmatic EMG. Blood gases were kept in the following ranges throughout the whole experiment: pH 7.50 ± 0.08 (range 7.38–7.63), P_{O_2} 141 ± 9.3 (range 122–159), P_{CO_2} 22.7 ± 5.9 (range 14–31). MABP was 108 ± 12 mmHg (range 102–113 mmHg). No significant changes in blood gases or MABP were detected under any experimental condition ($P > 0.05$). The bladder was cannulated to allow free flow of urine. Core temperature was maintained at 36.0–36.5°C using a thermostatically controlled heating blanket and was monitored using a thermocouple inserted into the colon.

Lumbar I.T. catheterization

Animals were fixed in a stereotaxic head-frame. The lower lumbar vertebrae were exposed and the L4 spinous process was clamped. The animal was made slightly kyphotic by gently lifting the clamp attached to the vertebra. The left inferior articular facet corresponding to L4 was removed and the ligamentum flavum incised. The dura was punctured with a 23 G × 11/4 in needle. Cerebrospinal fluid outflow indicated a subarachnoid position. A 32 G PU catheter (10 cm long, o.d. 0.0107 in and i.d. 0.005 in; Micor, Allison Park, PA, USA), reinforced with a Teflon-coated stainless steel stylet (0.003 in), was advanced rostrally (4.3 cm) through the needle (Pogatzki *et al.* 2000). The tip of the catheter was positioned at L1, as sympathetic preganglionic neurones supplying the tail circulation are distributed in the intermediolateral cell column between T11 and L2 and concentrated in L1–L2 (Smith & Gilbey, 1998). The needle was then removed and cyanoacrylate (Loctite superglue) was used to fix the catheter to the fascia.

In situ 'isolated' spinal cord preparation

The preganglionic neurones regulating SNAT were isolated from descending inputs by transecting the spinal cord between T10 and T11. Afferent and somatomotor axons arising from spinal segments below L5 were sectioned by cutting the cauda equina at the level between vertebrae L5 and L6 (see Supplemental Material).

The lower thoracic and lumbar vertebrae were exposed. The synovial ligaments between T9 and T10 and between L5 and L6 were cut, and the right and left facet joints were removed. Rats were neuromuscularly blocked and the cord and the cauda equina were transected. Bleeding was minimal and the cavity was packed with moist cotton wool.

Electrophysiological recording and data acquisition

Activity was recorded from the left dorsal collector nerve (DCN) as an index of SNAT. DCNs contain both sympathetic and somatic motor axons. However, only sympathetic activity was recorded from these nerves as somatomotor innervation of the tail had been decentralized (i.e. somatomotor efferents sectioned) by cutting the cauda equina (see Smith *et al.* 1998 and Supplemental Material). Population sympathetic activity was recorded using a suction electrode (Huang & Gilbey, 2005). The nerve was cut, desheathed and drawn into the electrode by applying negative pressure. Nerve activity was recorded through a high impedance headstage (NL 100, Neurolog; Digitimer Ltd, UK), preamplified (× 20000; NL 104, Neurolog), filtered (80–1000 Hz; NL 25, Neurolog) and amplified (× 20). Nerve activity was then

rectified and smoothed with a time constant of 100 ms (NL 703, Neurolog).

Nerve discharges, blood pressure, tracheal pressure and diaphragmatic EMG were monitored continuously on an IBM compatible computer (Dell, UK) using a 1401 plus interface and Spike2 software (Cambridge Electronic Design, UK) and digital storage oscilloscopes (VG-6023, Hitachi, Japan). For offline analysis nerve activity (prior to rectification and smoothing) and pressure signals (only for recording on tape) were sampled at approximately 11 kHz and stored on videotape and/or as a Spike2 data file. The sympathetic efferent nature of 5-HT or NMDA-induced nerve activity was confirmed in each experiment by its abolition following ganglionic blockade with trimetaphan camsylate (Cambridge Laboratories Limited, UK; 50 mg kg^{-1} I.V.) (see Chang *et al.* 1999 and Supplemental Material).

Experimental protocols

I.T. injections were performed using a 50 μl Hamilton syringe. Drugs were delivered with a microinjection pump (kd Scientific, model 100) at 120 $\mu l\,h^{-1}$ (10 μl followed by 2 μl of physiological saline). Sixty minutes after SCT, one of the following protocols was pursued: Experiment 1: DCN activity was monitored for 4 h without any further intervention ($n = 3$). Experiment 2: Animals received either 250 nmol of 5-HT (serotonin hydrochloride (Aldrich) pH 4.8, or serotonin creatinin sulphate complex (Sigma) pH 3.1, dissolved in physiological saline ($n = 6$)). Experiment 3: Animals received 1 μmol of NMDA ((Tocris) pH 3.0, dissolved in artificial cerebrospinal fluid ($n = 3$)). Experiment 4: Animals received 1 μmol of NMDA, and 30 min later, 250 nmol of 5-HT ($n = 6$). A further dose of 5-HT (250 nmol, I.T.) was administered 30 min after 5-HT-induced rhythmic activity had subsided. Data were pooled as similar results were obtained with both types of serotonin. The systemic administration of 5-HT (250 nmol I.V., $n = 4$) and the I.T. application of artificial cerebrospinal fluid or saline at pH 3 or 4.8, respectively, in spinalized animals did not have any effect on DCN activity. The doses of 5-HT and NMDA were the same as those used in other studies (Yusof & Coote, 1988; Chau *et al.* 2002). At the end of the experiments, animals were killed with an overdose of urethane. The location of the I.T. catheter and the completeness of SCT were verified.

Data analysis

Data were divided into 300 s sets. MABP was calculated in each set (diastolic $+1/3$(systolic $-$ diastolic)). DCN mean levels of activity were assessed for each data set following smoothing with a time constant of 10 s (Spike 2 software). Drug-induced changes in mean level of activity were normalized with respect to the pretransection level (100%). Zero was taken as that seen following SCT. Latency and duration of response were taken at the points where mean level of activity started to increase or returned to zero, respectively.

The frequency of the T-rhythm was assessed using frequency domain analysis. Data files were converted into text files and analysed using Matlab computer software (Maths Works). Dominant rhythm was assessed for each data set of rectified and smoothed activity (time constant 100 ms, sampled at 100 Hz). Fast Fourier transformation (FFT; size 2048, 50% overlap) was then performed. This divided the data sets into 28 half-overlapped 20.48 s long subsections with 2048 data points in each, giving a frequency resolution of 0.049 Hz. DC components and linear trends were then removed from the subsections. An autospectrum was averaged from these 28 subsections according to the Welch Method (see Chatfield, 1996). A dominant peak was allocated to an autospectrum where the envelope of spectral density that the peak was associated with, increased by more than 50% over six bins (0.3 Hz; see Smith & Gilbey, 2000).

Time-evolving autospectra were generated to examine temporal changes in DCN activity. The time-evolving spectrum was plotted as frequency against time (sequential data set number). Data were divided into 300 s subsections, and spectral analysis was performed on each subsection as described above. The absolute power density was normalized by its maximal value across time and its magnitude was then coded using a 64-grade colour scale. Changes in the colour scale represent the change of the power density across the recording time and the frequency range (see Chang *et al.* 1999).

Statistical analysis

Only those animals that displayed robust rhythmic discharges for 30 min in intact conditions were considered for statistical comparisons. All data sets with rhythmic activity were included in the analysis. Values for dominant frequency and percentage power in the dominant peak were averaged in each condition. The development of 5-HT-induced rhythmic activity was assessed by plotting the mean frequency with respect to its corresponding mean level of activity at five specific data sets: (1) after SCT, (2) first data set with robust rhythmicity, (3) highest mean level of activity, (4) last data set with rhythmicity and, (5) no rhythmicity. Results are expressed as mean $\pm$ S.E.M. One-way ANOVA was used to assess statistical significance in frequency between data sets; P values < 0.05 were considered significant.

Results

Sympathetic activity was recorded from the left DCN. Figures 1 and 2 show data from single experiments and group data are shown in Fig. 3.

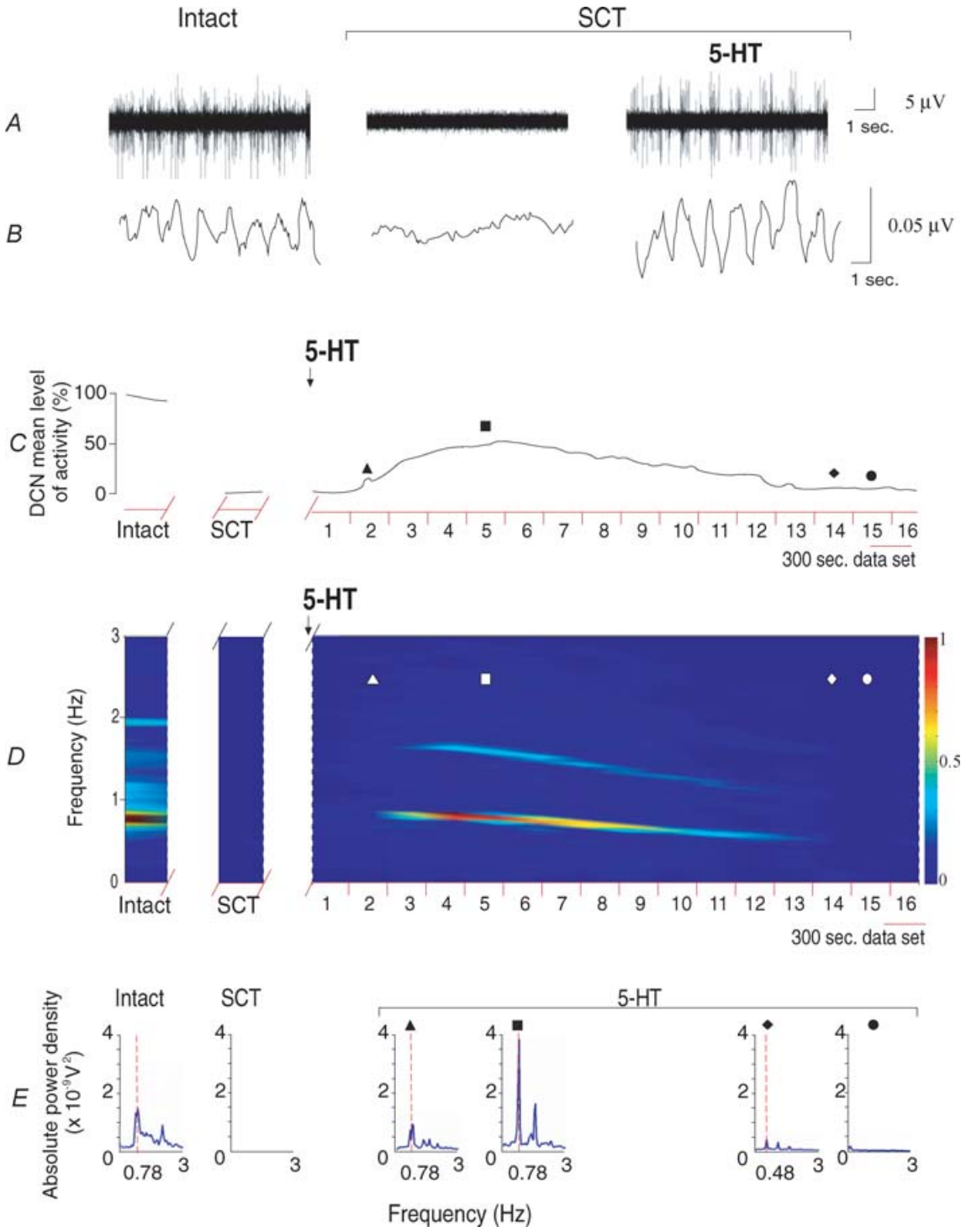

Figure 1. Intrathecal application of 5-HT (250 nmol) in a rat with spinal cord transection (SCT) induced robust rhythmic sympathetic activity similar to the physiological T-rhythm

A, raw and *B*, rectified and smoothed (time constant 100 ms) DCN neurograms. *C*, DCN mean level of activity (time constant 10 s). The data were divided into 300 s subsections. *D*, time-evolving autospectra of the DCN from the same animal and across the same time periods as in *C*. Spectral analysis was performed on each data set. The relative power density across time is coded by a 64-grade colour scale. *E*, 300 s data set power spectra in the intact animal and after spinal cord transection (SCT). The symbols highlight the power spectra taken at 4 specific data sets during the response to 5-HT, i.e. first data set with robust rhythmicity (▲), highest mean level of activity (■), last data set with rhythmicity (♦) and no rhythmicity (●). In the intact animal the DCN neurogram shows burst discharges with variable frequency and amplitude, and the autospectra are dominated by a band and a peak

Intact

As observed previously (Chang *et al.* 1999), DCN activity in intact animals displayed robust rhythmic discharges with variable frequency and amplitude (Figs 1 and 2; *A* and *B*). Frequency domain analysis showed a band in the time evolving autospectrum and a dominant peak in the power spectrum at 0.77 ± 0.02 Hz ($n = 16/18$, see Figs 1 and 2; *D* and *E*). In some cases, a lung inflation cycle-related component at 2 Hz was also observed ($n = 11/18$ see Figs 1 and 2; *D* and *E*). DCN autospectra did not reveal rhythmic components in 2 of 18 experiments.

Effect of SCT

SCT abolished SNAT (Fig. 1*A* and *B*; $n = 18$); the mean level of activity was similar to that observed after ganglionic blockade or neuronal death (i.e. zero level, Fig. 1*C*). Three animals were monitored for 4 h and no spontaneous recovery of SNAT was observed.

Effect of 5-HT on SNAT. Application of 5-HT (250 nmol, I.T.) 60 min after SCT induced robust rhythmic discharges (see Fig. 1*A* and *B*; $n = 6$). The latency was 5.3 ± 0.6 min (range 2–7 min) and the duration was 103 ± 12.6 min (range 55–145 min; see Fig. 1*C*). T-like rhythm frequencies showed two phases that were correlated with the changes in the mean level of activity. In the 'accelerating' phase, the mean level of activity increased and activity became rhythmic. The first data set with robust rhythmicity (see Fig. 1*D* and *E*, triangle) showed a band and a dominant peak in the autospectrum at 0.86 ± 0.04 Hz with its first harmonic peak at 1.72 ± 0.08 Hz (Fig. 3*A*) and had a mean level of activity of $57.3 \pm 28.6\%$ (range 4.1–135%, Fig. 3*A*); the highest mean level of activity induced by 5-HT was $174 \pm 67.7\%$ and showed a band and a dominant peak in the autospectra at 0.88 ± 0.04 Hz with its first harmonic peak at 1.76 ± 0.08 Hz (Fig. 3*A*, see also Fig. 1*D* and *E*, square). In 4 of 6 animals, the highest level of activity induced by 5-HT was lower than the level observed in the intact condition; in 2 of 6 animals, the level was higher (range 60.8–340%, see Fig. 1*C*). In the 'decelerating' phase, the frequency of the T-like rhythm slowed (see Fig. 1*D*) as the mean level of activity decreased (see Fig. 1*C*); the last data set with rhythmicity (see Fig. 1*C*–*E*, diamond) showed a band and a dominant peak in the autospectra at 0.65 ± 0.05 Hz with its first harmonic peak at 1.30 ± 0.10 Hz (Fig. 3*A*) and had a mean level of activity of $44.9 \pm 25.2\%$ (range 4–138%). This frequency was significantly slower than the frequency seen in the first data set with rhythmicity; however, the mean level of activity was similar in both data sets (Fig. 3*A*). No rhythmic components were seen in the following data set (see Fig. 1*C*–*E*, circle) where the mean level of activity was $42.2 \pm 19.4\%$ (range 4–132%; Fig. 3*A*). In all the cases, nerve activity ceased 10–15 min later and returned to SCT level. In all the cases, nerve activity ceased 10–15 min later. This suggests that rhythmogenic mechanisms dissipate slowly and the rhythm becomes weaker until it can no longer be detected at a population level.

Effect of NMDA on SNAT. In contrast, NMDA application (1 μmol I.T.) generated an irregular tonic activity (Fig. 2*A* and *B*, $n = 9$). We did not observe rhythmic discharges in the frequency range obtained with 5-HT (see Fig. 2*D* and *E*), even though a significant difference was not detected in the mean levels of activity induced by both drugs (compare Fig. 3*A* and *B*). The latency was 2.8 ± 1.3 min (range 1–5 min); the highest mean level of activity (see Fig. 2*C*, circle) was $99.1 \pm 26\%$ (Fig. 3*B*). In 4 of 9 animals, the highest level of activity induced by NMDA was lower than the level observed in the intact condition; in 5 of 9 animals, the level was higher (range 17–157%). The highest level of activity was sustained for a few seconds and then dropped to $31.4 \pm 9.9\%$, i.e. stable mean level of activity (range 12–69%; Fig. 3*B*; see also Fig. 2*C*, square). Three animals were monitored for 4 h with no further manipulation; activity was sustained and remained stable, but no rhythmic components were seen on the DCN autospectra.

Effect of 5-HT applied after NMDA. In six experiments 5-HT (250 nmol, I.T.) was applied 30 min after NMDA-induced tonic activity had stabilized; mean level of activity remained unchanged after 5-HT administration but tonic activity became rhythmic (see Fig. 2*A*–*C*). The latency was 26.4 ± 9.7 min and the duration was 18 ± 4.7 min (range 5–30 min). The first data set with rhythmicity (see Fig. 2*D* and *E*, triangle) showed a band and a dominant peak in the autospectra at 0.98 ± 0.13 Hz (Fig. 3*B*) and coincided with the highest mean level of activity induced by 5-HT ($77 \pm 27.9\%$, range 26.9–169%,

at 0.78 Hz (and a lung inflation cycle-related component at 2 Hz). SNAT was completely abolished after SCT; mean level of activity dropped to zero and rhythmical components are no longer observed in the autospectra. The I.T. administration of 5-HT induced robust rhythmic discharges. Note that DCN frequency changed with regard to the mean level of activity: the first data set with rhythmicity (▲) and the data set with the highest level of activity (■) were dominated by a band and a peak in the autospectra at 0.78 Hz with its first harmonic peak at 1.56 Hz. The last data set with rhythmicity (♦) showed a peak at 0.48 Hz and its first harmonic at 0.96 Hz. Rhythmic components were no longer observed in the following data set (●).

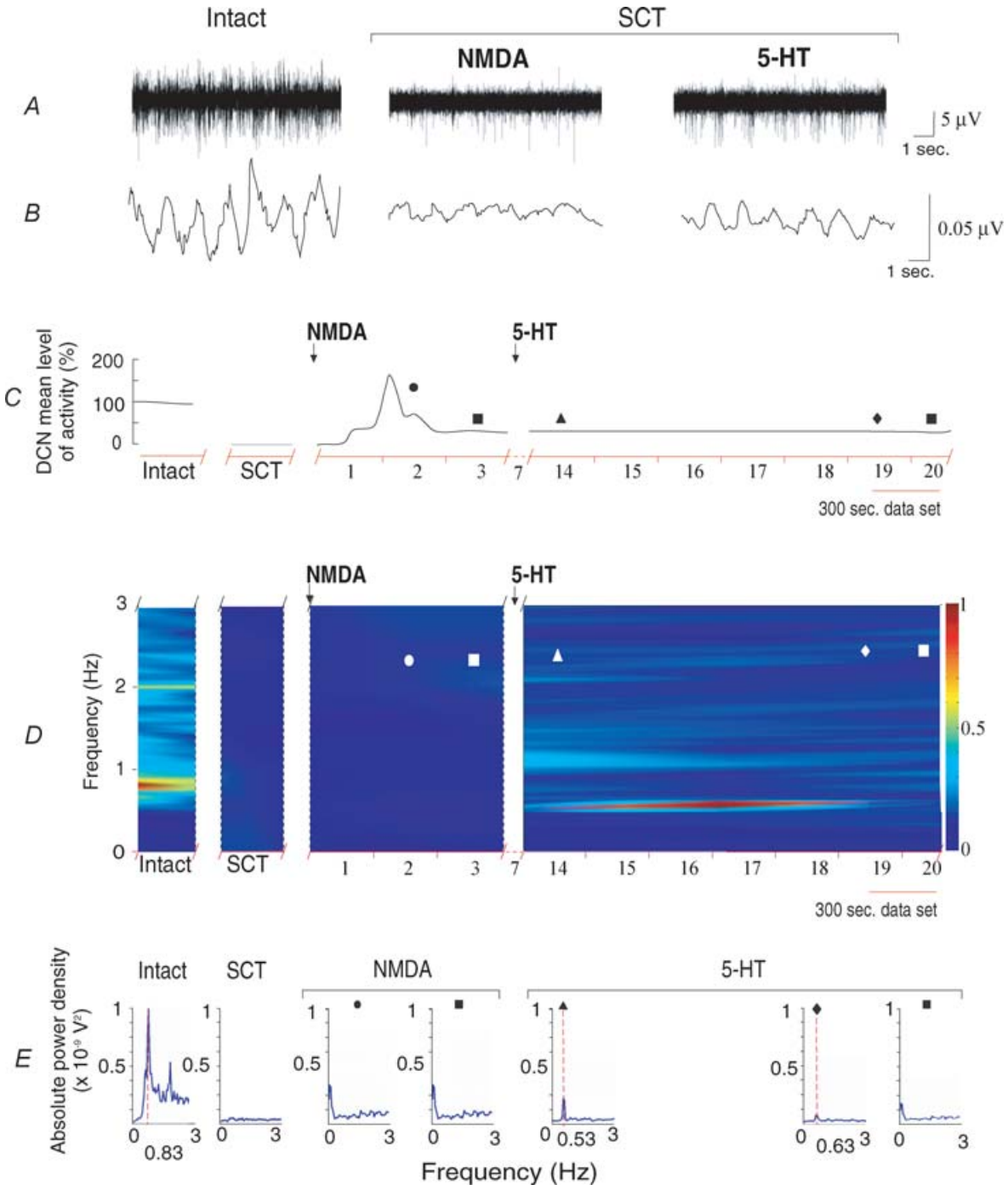

Figure 2. Intrathecal application of NMDA (1 μmol) in a rat with spinal cord transection (SCT) induced tonic sympathetic activity

The same as Fig. 1. The symbols highlight the power spectra taken at 5 specific data sets during the response to NMDA, i.e. highest and stable mean level of activity (● and ■, respectively) and 5-HT, i.e. first data set with robust rhythmicity (▲), last data set with rhythmicity (♦) and no rhythmicity (■). In the intact animal the DCN neurogram shows burst discharges with variable frequency and amplitude, and the autospectra is dominated by a band and a peak at 0.83 Hz (and a lung inflation cycle-related component at 2 Hz). Mean level of activity dropped to zero after SCT and rhythmical components were no longer observed in the autospectra. The I.T. administration of NMDA generated an irregular tonic activity. The mean level of activity increased 152% (●), and dropped rapidly, remaining stable at 29% (■). DCN autospectra showed a peak with very low frequency (0.07 Hz) during these two phases. A dose of 5-HT (250 nmol, I.T.) was administered 30 min after NMDA-induced activity was stable; mean level of activity remained unchanged after 5-HT administration but tonic activity became rhythmic during 6 data sets. The

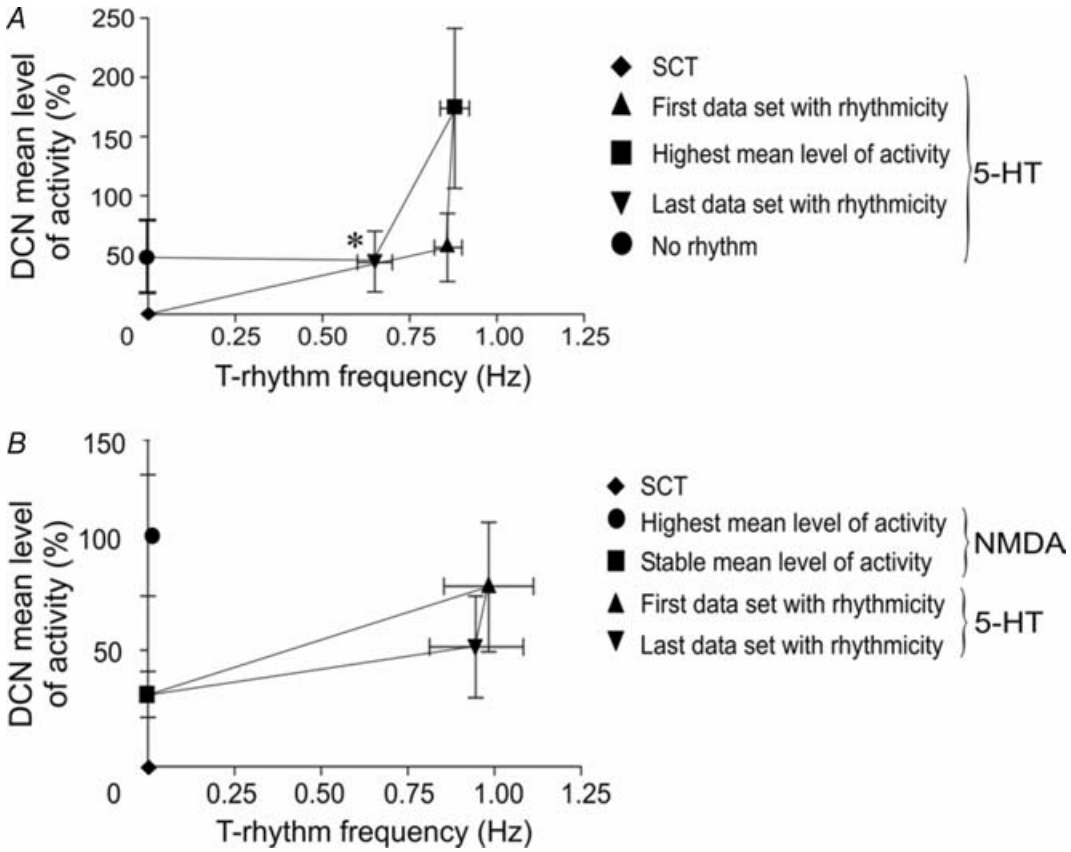

Figure 3. T-like rhythm frequency with relation to the mean level of activity
Response to 5-HT and NMDA + 5-HT in animals with spinal cord transection (SCT). *A*, 5-HT response. The frequency of the T-like rhythm was similar during the first data set with rhythmicity and the highest mean level of activity. Note that the frequency in the last data set with rhythmicity is significantly slower even though the level of activity is similar to the first data set. *B*, NMDA + 5-HT response. Spectral analysis showed no rhythmic components in response to NMDA application. The mean levels of activity induced by NMDA and 5-HT alone (*A*) were not significantly different (highest *versus* highest and stable *versus* first/last data set with rhythmicity, respectively). However, a T-like rhythm appeared when 5-HT was administered without producing significant changes in the mean level of activity. The frequency of the T-rhythm was stable and no significant differences were observed in the first and last data sets with rhythmicity. Results are expressed as mean ± S.E.M. One-way ANOVA was used to analyse statistical differences in T-like rhythm frequency between data sets. $^*P < 0.05$.

Fig. 3*B*); the last data set with rhythmicity (see Fig. 2*D* and *E*, diamond) showed a dominant peak in the autospectra at 0.94 ± 0.10 Hz (Fig. 3*B*) and had a mean level of activity of 65.1 ± 29.8% (range 5.92–197%). Rhythmic discharge frequencies in the first and the last segments were not significantly different. Following the cessation of rhythmic activity SNAT returned to the irregular tonic state (see Fig. 2*D* and *E*, square).

In all the cases, it was possible to initiate sequences of rhythmic activity by performing further applications of 5-HT. The frequencies of rhythmic activity induced by 5-HT or NMDA + 5-HT in spinalized animals were not significantly different from those observed before SCT. However, percentage power in the dominant peak induced by 5-HT alone (155.6 ± 38.7% relative to pretransection) was significantly higher than the power observed with NMDA + 5-HT (31.8 ± 8.8%).

Discussion

In this study we have demonstrated that a 'dominant' physiological sympathetic motor rhythm (i.e. T-rhythm) can be reproduced following I.T. application of 5-HT to an *in situ* 'isolated' spinal cord preparation. Whereas 5-HT was effective, treatment with NMDA failed to reproduce the rhythm, although a significant difference in the level

first (▲) and the last (♦) data sets with rhythmicity showed a peak and a band in autospectra at 0.53 Hz and 0.63 Hz, respectively. Rhythmic components were no longer observed in the following data sets (■) and activity returned to the tonic state and remained stable for 3 h until the animal was killed.

of activity produced by both drugs was not detected. These differential actions of 5-HT and NMDA counter the argument that rhythmic activity is generated by postganglionic neurones in response to 'tonic' drive and indicate that the T-rhythm can be generated within the spinal cord. Therefore the spinal cord may be an important site for sympathetic rhythm generation (in addition to the brain stem; see Barman & Gebber, 2000). We consider that this study is important as it has provided data that link observations made *in vitro* that reveal the actions of 5-HT at the cellular level on sympathetic preganglionic neurones (Pickering *et al.* 1994) and the so-called T-rhythm studied in intact anaesthetized preparations (Gilbey, 2001).

Sympathetic neuronal activity to the tail (SNAT) is driven by descending excitatory inputs from rostral ventromedial medulla

We demonstrated that SNAT was abolished after T10–T11 spinal cord transection: a critical amount of this drive appears to arise from the rostral ventromedial medulla (Tanaka *et al.* 2002; Korsak & Gilbey, 2004; Ootsuka *et al.* 2004; Ootsuka & Blessing, 2005; Ootsuka & McAllen, 2005). In contrast, ongoing sympathetic activity to other cardiovascular outflows (i.e. heart and kidney) relies vitally upon supraspinal drive from the rostral ventrolateral medulla (Horiuchi *et al.* 2004).

5-HT generates rhythmic sympathetic motor activity

Some neurones within the RVMM that innervate tail sympathetic preganglionic neurones demonstrate 5-HT-like immunoreactivity (Smith *et al.* 1998). Therefore our findings are consistent with the contention that the T-rhythm is generated by a direct action of 5-HT upon receptors located on sympathetic preganglionic neurones. When sympathetic preganglionic neurones are in 'oscillator' mode, inputs may reset or entrain the T-rhythm (Gilbey, 2001; Staras *et al.* 2001). For example, central respiratory-related inputs may entrain these 'oscillators', consistent with the 'entrainment hypothesis'. In contrast, when sympathetic preganglionic neurones have a tonic firing pattern, central respiratory-related inputs may produce rhythmic sympathetic neuronal discharges through a modulation of tonic activity, consistent with a 'radiation hypothesis' (see Gilbey, 2004). Therefore, 'entrainment of sympathetic oscillators' and 'radiation' hypotheses are not mutually exclusive.

The rhythmogenic effect of 5-HT can be explained both by intrinsic membrane properties in individual neurones and by network mechanisms. It has been shown that 5-HT can generate rhythmic subthreshold membrane potential oscillations in single sympathetic preganglionic neurones from thoracic and lumbar segments (Pickering *et al.* 1994). The time course of the response obtained *in vitro* was slow in onset and prolonged in duration, as we observed *in vivo*. This suggests that 5-HT is acting via a second messenger cascade. The longer latency to onset and longer response duration that we observed *in vivo*, compared with a slice preparation, may be explained by a longer diffusion distance and by a longer application and contact time. Extracellular recordings in intact animals have also shown that 5-HT can induce a rhythmic firing pattern in irregularly discharging sympathetic preganglionic neurones (Lewis & Coote, 1996). At the network level, there is evidence of electrotonic coupling through gap junctions between sympathetic preganglionic neurones with spontaneous membrane oscillations in neonatal and adult rats (Logan *et al.* 1996; Leslie *et al.* 2000). It is well known that gap junction coupling can be modified by endogenously released neurotransmitters, such as 5-HT (Rorig & Sutor, 1996). Therefore, by regulating gap junction coupling, 5-HT may influence the degree of synchrony in the discharges of the population, causing recruitment of more neurones and enable electrotonic transmission of the oscillations.

NMDA generates tonic sympathetic motor activity

Although NMDA failed to elicit a T-like rhythm in our preparation, it generated a tonic activity which remained stable for at least 4 h. This is the first time that such a long-lasting effect of NMDA has been observed in sympathetic preganglionic neurones *in vivo* and requires further investigation. *In vitro* experiments have shown that EPSPs recorded from sympathetic preganglionic neurones are potentiated following a brief high-frequency stimulus (Spanswick *et al.* 1998), a protocol often employed to induce long-term potentiation (LTP) in the hippocampus which involves the activation of NMDA receptors. The potentiation of the EPSPs observed in the latter study also had a long time course and it was sustained over the time course of recording.

Chizh *et al.* (1998) observed that NMDA applied through the circulatory system of an arterially perfused trunk–hindquarters preparation of adult mouse induced common rhythms in sympathetic discharge (renal nerve and abdominal sympathetic chain) and somatomotor activity. These authors suggested that these common rhythms were produced by the somatomotor rhythm generator pervading the sympathetic circuits and were quite distinct from 'spinal sympathetic rhythm' generators. Our observation that NMDA failed to produce rhythmic activity in the sympathetic outflow argues against the T-rhythm arising from a common somato-sympathetic rhythm generator.

Although NMDA-induced tonic activity became rhythmic when 5-HT was subsequently administered, the rhythm was less strong than the rhythm induced by 5-HT alone. Therefore, it appears that the tonic activity induced

by NMDA interferes with the rhythmicity induced by 5-HT.

The findings of Ootsuka & Blessing (2005; ear pinna, rabbit) support the idea that excitatory amino acid and 5-HT-mediated inputs, originating from the RVMM, influence cutaneous sympathetic vasomotor activity. These authors demonstrated that application of a selective 5-HT_{2A} antagonist to the spinal cord reduced raphé-evoked increases in sympathetic activity and the remaining evoked discharge was substantially further reduced by the application of kynurenate.

Conclusions

We consider that this study is important as it bridges observations made in animals with intact nervous systems (see Gilbey, 2001) and those made in the *in vitro* slice preparation (i.e. see Pickering *et al.* 1994). It provides a vital systems perspective on detailed mechanistic data acquired from single cell recordings and raises the possibility that a sympathetic vasomotor rhythm is generated within the spinal cord.

References

Alford S, Schwartz E & Viana di Prisco G (2003). The pharmacology of vertebrate spinal central pattern generators. *Neuroscientist* **3**, 217–228.

Arshavsky YI (2003). Cellular and network properties in the functioning of the nervous system: from central pattern generators to cognition. *Brain Res Brain Res Rev* **41**, 229–267.

Barman SM & Gebber GL (2000). 'Rapid' rhythmic discharges of sympathetic nerves: sources, mechanisms of generation, and physiological relevance. *J Biol Rhythms* **15**, 365–379.

Buzsáki G & Draguhn A (2004). Neuronal oscillations in cortical networks. *Science* **304**, 1926–1929.

Chang HS, Staras K & Gilbey MP (2000). Multiple oscillators provide metastability in rhythm generation. *J Neurosci* **20**, 5135–5143.

Chang HS, Staras K, Smith JE & Gilbey MP (1999). Sympathetic neuronal oscillators are capable of dynamic synchronization. *J Neurosci* **19**, 3183–3197.

Chatfield C (1996). *The Analysis of Time Series*. Thomson Science and Professional, London.

Chau C, Giroux N, Barbeau H, Jordan L & Rossignol S (2002). Effects of intrathecal glutamatergic drugs on locomotion I. NMDA in short-term spinal cats. *J Neurophysiol* **88**, 3032–3045.

Chizh BA, Headley PM & Paton JF (1998). Coupling of sympathetic and somatic motor outflows from the spinal cord in a perfused preparation of adult mouse *in vitro*. *J Physiol* **508**, 907–918.

Collins DR & Gilbey MP (2003). Cutaneous sympathetic motor rhythms in the decerebrate rat. *Neuroscience* **117**, 981–989.

Douglas JR, Noga BR, Dai X & Jordan LM (1993). The effects of intrathecal administration of excitatory amino acid agonists and antagonists on the initiation of locomotion in the adult cat. *J Neurosci* **13**, 990–1000.

Fedirchuk B, Nielsen J, Petersen N & Hultborn H (1998). Pharmacologically evoked fictive motor patterns in the acutely spinalized marmoset monkey (*Callithrix jacchus*). *Exp Brain Res* **122**, 351–361.

Gilbey MP (2001). Multiple oscillators, dynamic synchronization and sympathetic control. *Clin Exp Pharmacol Physiol* **28**, 130–137.

Gilbey MP (2004). Entrainment of sympathetic rhythms. In *Primer on the Autonomic Nervous System*, ed. Robertson P, pp. 114–115. Graph World Publishing Services, St Louis.

Horiuchi J, McAllen RM, Allen AM, Killinger S, Fontes MA & Dampney RA (2004). Descending vasomotor pathways from the dorsomedial hypothalamic nucleus: role of medullary raphe and RVLM. *Am J Physiol Regul Integr Comp Physiol* **287**, 824–832.

Huang C & Gilbey MP (2005). A comparison of simultaneously recorded muscle and skin vasoconstrictor population activities in the rat using frequency domain analysis. *Auton Neurosci* **121**, 47–55.

Johnson CD & Gilbey MP (1994). Sympathetic activity recorded from the rat caudal ventral artery *in vivo*. *J Physiol* **476**, 437–442.

Johnson CD & Gilbey MP (1996). On the dominant rhythm in the discharges of single postganglionic sympathetic neurones innervating the rat tail artery. *J Physiol* **497**, 241–259.

Korsak A & Gilbey MP (2004). Rostral ventromedial medulla and the control of cutaneous vasoconstrictor activity following i.c.v. prostaglandin E(1). *Neuroscience* **124**, 709–717.

Leslie J, Nolan MF, Logan SD & Spanswick D (2000). Electrotonic coupling between sympathetic preganglionic neurons in neonatal and adult rat *in vitro*. *J Physiol* **582.P**, 108*P*.

Lewis DI & Coote JH (1996). Evidence that the firing pattern of sympathetic preganglionic neurons is determined by an interaction between amines and an excitatory aminoacid. *Boll Soc Ital Biol Sper* **72**, 279–294.

Logan SD, Pickering AE, Gibson IC, Nolan MF & Spanswick D (1996). Electrotonic coupling between rat sympathetic preganglionic neurones *in vitro*. *J Physiol* **495**, 491–502.

Malpas SC (1998). The rhythmicity of sympathetic nerve activity. *Prog Neurobiol* **56**, 65–96.

Marina N & Gilbey MP (2005*a*). Sympathetic motor rhythms are generated within the spinal cord in response to serotonin. *J Physiol* **567P**, PC47.

Marina N & Gilbey MP (2005*b*). Generation of sympathetic motor rhythms in the spinal cord by serotonin. *Abstr Soc Neurosci* 753.6.

Nakamura Y, Katakura N, Nakajima M & Liu J (2004*a*). Rhythm generation for food-ingestive movements. *Prog Brain Res* **143**, 97–103.

Nakamura K, Matsumura K, Hubschle T, Nakamura Y, Hioki H, Fujiyama F *et al.* (2004*b*). Identification of sympathetic premotor neurons in medullary raphe regions mediating fever and other thermoregulatory functions. *J Neurosci* **24**, 5370–5380.

Ootsuka Y & Blessing WW (2005). Activation of slowly conducting medullary raphe-spinal neurons, including serotonergic neurons, increases cutaneous sympathetic vasomotor discharge in rabbit. *Am J Physiol Regul Integr Comp Physiol* **288**, 909–918.

Ootsuka Y, Blessing WW & McAllen RM (2004). Inhibition of rostral medullary raphe neurons prevents cold-induced activity in sympathetic nerves to rat tail and rabbit ear arteries. *Neurosci Lett* **357**, 58–62.

Ootsuka Y & McAllen RM (2005). Interactive drives from two brain stem premotor nuclei are essential to support rat tail sympathetic activity. *Am J Physiol Regul Integr Comp Physiol* **289**, R1107–R1115.

Peña F & Ramirez JM (2002). Endogenous activation of serotonin-2A receptors is required for respiratory rhythm generation *in vitro*. *J Neurosci* **22**, 11055–11064.

Pickering AE, Spanswick D & Logan SD (1994). 5-Hydoxytryptamine evokes depolarizations and membrane potential oscillations in rat sympathetic preganglionic neurones. *J Physiol* **480**, 109–121.

Pogatzki EM, Zahn PK & Brennan TJ (2000). Lumbar catheterization of the subarachnoid space with a 32-gauge polyurethane catheter in the rat. *Eur J Pain* **4**, 111–113.

Rathner JA, Owens NC & McAllen RM (2001). Cold-activated raphe-spinal neurons in rats. *J Physiol* **535**, 841–854.

Rorig B & Sutor B (1996). Serotonin regulates gap junction coupling in the developing rat somatosensory cortex. *Eur J Neurosci* **8**, 1685–1695.

Schmidt BJ & Jordan LM (2000). The role of serotonin in reflex modulation and locomotor rhythm production in the mammalian spinal cord. *Brain Res Bull* **53**, 689–710.

Singer W (1993). Synchronization of cortical activity and its putative role in information processing and learning. *Annu Rev Physiol* **55**, 349–374.

Smith JE & Gilbey MP (1998). Segmental origin of sympathetic preganglionic neurones regulating the tail circulation in the rat. *J Auton Nerv Syst* **68**, 109–114.

Smith JE & Gilbey MP (2000). Coherent rhythmic discharges in sympathetic nerves supplying thermoregulatory circulations in the rat. *J Physiol* **523**, 449–457.

Smith JE, Jansen AS, Gilbey MP & Loewy AD (1998). CNS cell groups projecting to sympathetic outflow of tail artery: neural circuits involved in heat loss in the rat. *Brain Res* **786**, 153–164.

Spanswick D, Renaud LP & Logan SD (1998). Bilaterally evoked monosynaptic EPSPs, NMDA receptors and potentiation in rat sympathetic preganglionic neurones *in vitro*. *J Physiol* **509**, 195–209.

Staras K, Chang HS & Gilbey MP (2001). Resetting of sympathetic rhythm by somatic afferents causes post-reflex coordination of sympathetic activity in rat. *J Physiol* **533**, 537–545.

Tanaka M, Nagashima K, McAllen RM & Kanosue K (2002). Role of the medullary raphe in thermoregulatory vasomotor control in rats. *J Physiol* **540**, 657–664.

Ward LM (2003). Synchronous neural oscillations and cognitive processes. *Trends Cogn Sci* **12**, 553–559.

Yusof AP & Coote JH (1988). Excitatory and inhibitory actions of intrathecally administered 5-hydroxytryptamine on sympathetic nerve activity in the rat. *J Auton Nerv Syst* **22**, 229–236.

Acknowledgements

This work was supported by the Wellcome Trust (grant number 063954). M.T. was a BSc project student in our laboratory and received a vacational studentship from The Physiological Society.

Supplemental material

The online version of this paper can be accessed at:
DOI: 10.1113/jphysiol.2005.100677
http://jp.physoc.org/cgi/content/full/jphysiol.2005.100677/DC1
and contains two supplemental figures showing the isolated spinal cord preparation and ganglionic blockade.

This material can also be found as part of the full-text HTML version available from http://www.blackwell-synergy.com